

Quantum critical scaling at a Bose-glass/superfluid transition: theory and experiment on a model quantum magnet

Rong Yu,¹ Corneliu F. Miclea,^{2,3} Franziska Weickert,² Roman Movshovich,²
Armando Paduan-Filho,⁴ Vivien S. Zapf,² and Tommaso Roscilde⁵

¹*Department of Physics & Astronomy, Rice University, Houston, TX 77005, USA*

²*Condensed Matter and Magnet Science, Los Alamos National Lab, Los Alamos, NM 87545*

³*National Institute for Materials Physics, 077125 Bucharest-Magurele, Romania*

⁴*Instituto de Física, Universidade de São Paulo, 05315-970 São Paulo, Brasil*

⁵*Laboratoire de Physique, CNRS UMR 5672, Ecole Normale Supérieure de Lyon,
Université de Lyon, 46 Allée d'Italie, Lyon, F-69364, France*

In this paper we investigate the quantum phase transition from magnetic Bose glass to magnetic Bose-Einstein condensation induced by a magnetic field in $\text{NiCl}_2 \cdot 4\text{SC}(\text{NH}_2)_2$ (dichloro-tetrakis-thiourea-Nickel, or DTN), doped with Br (Br-DTN) or site diluted. Quantum Monte Carlo simulations for the quantum phase transition of the model Hamiltonian for Br-DTN, as well as for site-diluted DTN, are consistent with conventional scaling at the quantum critical point and with a critical exponent z verifying the prediction $z = d$; moreover the correlation length exponent is found to be $\nu = 0.75(10)$, and the order parameter exponent to be $\beta = 0.95(10)$. We investigate the low-temperature thermodynamics at the quantum critical field of Br-DTN both numerically and experimentally, and extract the power-law behavior of the magnetization and of the specific heat. Our results for the exponents of the power laws, as well as previous results for the scaling of the critical temperature to magnetic ordering with the applied field, are incompatible with the conventional crossover-scaling Ansatz proposed by Fisher *et al.*, [Phys. Rev. B **40**, 546 (1989)], but they can all be reconciled within a phenomenological Ansatz in the presence of a dangerously irrelevant operator.

PACS numbers: 03.75.Lm, 71.23.Ft, 68.65.Cd, 72.15.Rn

I. INTRODUCTION

The investigation of interacting bosons in the presence of randomness (the so-called *dirty-boson* problem) represents a long-standing subject in quantum condensed matter, and in particular a subject which remains far from being settled. Indeed disorder has a tremendous impact on the physics of bosons, introducing a significant richness in their phase diagram both at zero and at finite temperature. Intense experimental investigations on a wide variety of different physical systems – including ^4He in porous media¹, cold atoms in disordered optical potentials², and doped antiferromagnetic insulators³⁻⁶, among others – have been pursued in the attempt to unveil the universal aspects of such a phase diagram. A similarly intense activity has been conducted at the theoretical level⁷, using a variety of methods ranging from field theory to quantum Monte Carlo. Yet, despite more than two decades of intense investigation, fundamental aspects of the physics of dirty bosons remain obscure. Among the most salient aspects under debate are the nature of the non-condensed and non-superfluid state induced by disorder *and* interactions in a Bose fluid – namely the compressible Bose glass or the incompressible Mott glass; and the nature of the quantum phase transition (QPT) from a Bose glass to a strongly interacting superfluid Bose-Einstein condensate (BEC), induced by increasing the role of interactions while keeping the disorder strength fixed⁸. In particular, the latter transition does not admit a well-controlled analytical treatment, its critical exponents are generally unknown, and the existing predictions⁸ are highly debated⁹.

In this paper we address the problem of the Bose-glass/superfluid QPT from the point of view of a model mag-

net, $\text{NiCl}_{2(1-x)}\text{Br}_{2x} \cdot 4\text{SC}(\text{NH}_2)_2$ (Br-doped dichloro-tetrakis-thiourea-Nickel, or Br-DTN), whose magnetic Hamiltonian can be mapped exactly onto that of $3d$ interacting bosons on a lattice with random hopping and random on-site interactions. A recent experiment⁵ has demonstrated that this compound exhibits an extended magnetic Bose-glass phase in an applied magnetic field – such a phase is characterized by a gapless and magnetically disordered low-temperature state. Increasing the field beyond a critical value drives the system through a QPT from Bose glass to magnetic BEC, characterized by spontaneous long-range antiferromagnetism in the plane transverse to the field. In particular the critical temperature to condensation is shown to scale with the applied field as $T_c \sim |h - h_c|^\phi$ with $\phi = 1.1(1)$, where h represents the dimensionless magnetic field and h_c its critical value. A seemingly puzzling feature is that the only theoretical prediction for the ϕ exponent, stemming from Ref. 8, gives $\phi \geq 2$, in open contradiction with the result of Ref. 5. Using quantum Monte Carlo simulations of the model Hamiltonian for Br-DTN, as well as of the Hamiltonian of DTN with a diluted magnetic lattice, we provide a detailed investigation of the quantum critical scaling at the Bose-glass/superfluid transition. In the case of Br-DTN we also investigate the low-temperature specific heat – both numerically and experimentally – and the magnetization – numerically – around the critical field. Our theoretical data for the zero-temperature quantum critical point (QCP) support the picture of conventional scaling and the prediction⁸ of $z = d = 3$ for the dynamical critical exponent. Nonetheless the results for the behavior of the system at finite temperature are seen to be globally incompatible with the predictions stemming from the scaling Ansatz of Ref. 8 for the free energy, which assumes that the temperature is the only direction

of instability of the QCP, while disorder and interactions can be eliminated from the scaling. We discuss possible violations of conventional scaling, due to the presence of a dangerously irrelevant operator, and find that a fully consistent picture can only be obtained when assuming that such an operator affects the finite-temperature behavior only, preserving conventional scaling at $T = 0$. In the absence of a consistent theoretical treatment of the long-wavelength behavior of dirty bosons⁷, our results offer a first, empirical determination of the scaling behavior around the dirty-boson QCP.

The structure of the paper is as follows: Sec. II reviews the main aspects of the QPT of dirty bosons; Sec. III shortly illustrates how statically doped DTN realizes the physics of disordered lattice bosons; Sec. IV illustrates the crossover scaling Ansatz of Ref. 8 and its predictions for the quantum critical behavior; Sec. V discusses the numerical estimate of the dynamical critical exponent and of other critical exponents at the dirty-boson QCP; Sec. VI presents our numerical as well as experimental results for the thermodynamics of Br-DTN at the quantum critical field; Sec. VII discusses how all of our results can be captured quantitatively by a generalized scaling Ansatz; conclusions are drawn in Sec. VIII.

II. DIRTY-BOSON QUANTUM CRITICAL POINT

In the absence of disorder, the physics of interacting bosons is generally well understood following a set of established paradigms. A diluted Bose gas of weakly interacting bosons undergoes condensation in a spatially extended state, and it is quantitatively described by Bogolyubov and Beliaev theory¹⁰. The QPT from the vacuum state into the condensed state, driven by the chemical potential, represents a Gaussian transition in dimensions $d > 1$ with dynamical critical exponent $z = 2$.¹¹ In $d = 3$ the onset of the critical temperature to condensation around the QCP follows the power-law scaling $T_c \sim |\mu - \mu_c|^\phi$ (where μ_c is the critical chemical potential), with $\phi = 2/3$ as predicted by mean-field theory¹². For bosons on a lattice, an instability to the formation of a Mott-insulating state occurs for sufficiently large interactions, and the QPT from a superfluid condensate to a Mott insulator away from commensurate filling admits the same description as the QCP of the diluted Bose gas, while it belongs to the universality class of the XY model in $d + 1$ dimensions at commensurate filling.⁸

The introduction of disorder to the system is accompanied by the Anderson localization of the (low-energy) single-particle eigenstates; such states cannot host a Bose-Einstein condensate in the thermodynamic limit in the presence of any finite interaction. As a consequence, the physics of the diluted Bose gas is completely altered by disorder, and a novel phase appears - the bosonic Anderson glass or Bose glass^{8,13} - characterized by the redistribution of bosons on an extensive number of low-lying Anderson-localized states. This fact renders the theoretical description of the Bose glass quite involved, as conventional tools for the diluted Bose gas are no longer available. This is *a fortiori* true when the interaction strength increases (the disorder strength being held fixed), inducing a

QPT from the Bose glass into a strongly correlated condensed and superfluid state. This transition, as well as other transitions in disordered systems¹⁴, represents an exceptionally hard problem in the theory of critical phenomena. Indeed the upper critical dimension d_c , above which mean-field theory becomes exact, is unknown for dirty bosons; and perturbative renormalization group treatments break down⁸, given that they are based on the assumption of a finite d_c , while d_c might as well be infinity for dirty bosons. This means that a quantitative understanding of the behavior of interactions and disorder under renormalization is still lacking, as well as a rigorously motivated scaling form for the free energy. In the following we will offer evidence that the scaling Ansatz for the free energy proposed by Ref. 8 is not appropriate.

Another fundamental open question concerns the value of the dynamical critical exponent z . The derivation of the identity $z = d$ offered in Ref. 8 has been questioned in Ref. 9, and some numerical calculations in $d = 2$ seem indeed to contradict it^{15,16}, although other $2d$ studies are instead consistent with it¹⁷⁻²². For $d = 3$ much less results are available, but $z = 3$ is consistent with the existing numerical studies of the $3d$ Bose-glass/superfluid transition^{22,23}, and, as we will see, also with the numerical results of this work (Sec. V).

The derivation of $z = d$ in Ref. 8 is based on the observation that the compressibility $\kappa = \partial^2 f / \partial \mu^2$ (where f is the free energy density and μ is the chemical potential) behaves as the imaginary-time stiffness of the system. An expansion of the *singular* part of the free energy upon an infinitesimal twist leads to the prediction that $\kappa \sim g^{\nu(d-z)}$, where g is the distance to the critical point; if the compressibility is to remain finite across the transition, this would then imply that $d = z$. This derivation has been questioned by Ref. 9, on the basis that the main response to a twist in imaginary time is expected to come from the *analytical* rather than from the singular part of the free energy - this is due to the fact that, if the particle-hole symmetry is already broken (as it is across the generic Bose-glass/superfluid transition), a variation in the chemical potential does not alter the Hamiltonian symmetries in the system, and hence it should lead to negligible contributions in the singular part of the free energy density. Therefore the finiteness of κ across the transition should not have any obvious implication for the critical exponents.

It is generally hard to believe as an accident that many numerical results appear to be consistent with $z = d$ - although, as noticed in Ref. 16, only in a few cases an unbiased estimate of z has been provided. Without the pretension of solving the issue of the value of z , in the following we provide a simple derivation of the finite-size scaling for the compressibility at zero temperature, based on its relationship with the particle-hole gap. Indicating with $E(N)$ the ground-state energy of the system having N particles, we have that the particle-hole gap takes the form

$$\Delta_{\text{ph}} = E(N + 1) + E(N - 1) - 2E(N). \quad (1)$$

For an hypercubic system of size L^d , taking the limit $L, N \gg 1$ one obtains

$$\Delta_{\text{ph}} \approx \frac{\partial^2 E}{\partial N^2} = \frac{1}{L^d} \frac{1}{\kappa} \quad (2)$$

where we have used the fact that $\mu = \partial E / \partial N$, and the definition of the compressibility $\kappa = L^{-d} \partial N / \partial \mu$. At the QCP, the finite-size particle-hole gap must vanish as $\Delta_{\text{ph}} \sim L^{-z}$, yielding the result $\kappa \sim L^{-(d-z)}$. Hence a finite compressibility in the thermodynamic limit at the QCP would require that $z = d$. The above derivation is based on the only assumption that conventional scaling applies (giving $\Delta_{\text{ph}} \sim L^{-z}$), namely that the system is below or at the upper critical dimension. The scaling of κ is indeed observed at the commensurate-incommensurate transition of the Bose-Hubbard model with $z = 2$ both in $d = 1$ (where the compressibility diverges²⁴) and in $d = 2$ (where the compressibility jumps²⁷, up to logarithmic corrections). It is also verified at the Mott-insulator/superfluid transition at commensurability (with $z = 1$), *e.g.* in $d = 1$ (compressibility jump at the Kosterlitz-Thouless transition²⁴) and in $d = 2, 3$ (where the compressibility vanishes continuously^{25,26}).

III. DIRTY BOSONS AND THE PHYSICS OF DOPED DTN

Recently a new experimental playground has become available for the study of the physics of dirty bosons: doped magnetic insulators. In such systems a Bose fluid of magnetic quasiparticles (corresponding to modes carrying a spin $m_s = 1$) can be controlled by the application of a magnetic field, and can be made to condense at sufficiently low temperature when the field exceeds a critical value²⁸. The condensed phase corresponds to long-range (anti)ferromagnetism in the plane transverse to the field. Static doping of the magnetic insulator leads to disorder in the magnetic Hamiltonian, and allows therefore to investigate a field-induced Bose-glass/superfluid transition, which has been discussed theoretically^{5,20,29,30} as well as recently probed in experiments^{3-6,31,32}.

Here we focus our attention on Br-doped DTN, which has been recently investigated in Ref. 5. A minimal model Hamiltonian for the magnetic behavior of Br-DTN is given by

$$\begin{aligned} \mathcal{H}_{\text{Br-DTN}} = & \sum_{\langle ij \rangle_c} J_{c, \langle ij \rangle} \mathbf{S}_i \cdot \mathbf{S}_j + J_{ab} \sum_{\langle lm \rangle_{ab}} \mathbf{S}_l \cdot \mathbf{S}_m \\ & + \sum_i D_i (S_i^z)^2 - g\mu_B H \sum_i S_i^z. \end{aligned} \quad (3)$$

Here S_i^α ($\alpha = x, y, z$) are $S = 1$ spin operators, coupled on a cubic lattice with antiferromagnetic interactions J_c along the c axis and J_{ab} in the ab plane; D is a strong single-ion anisotropy. In pure DTN $J_c = 2.2$ K, $J_{ab} = 0.18$ K, $D = 8.9$ K and $g = 2.26$.³³ The effect of Br doping on the magnetic behavior can be quantitatively captured by promoting the J_c couplings and the single-ion anisotropies to local, bond-dependent ($J_{c, \langle ij \rangle}$) and site-dependent (D_i) quantities, related to the appearance of a Br dopant on the Cl-Cl bond bridging the antiferromagnetic interactions between Ni ions along the c axis. In particular a concentration x of Br dopants leads to a fraction $2x$ of doped Cl-Br bonds (neglecting the case of rare Br-Br bonds for $x \ll 1$); Br doping is modeled as increasing the J_c bond strength to $J'_c = 2.3J_c$, and reducing the single anisotropy D to $D' = D/2$ on one of the two ions

connected by the bond. In the rest of this paper we will focus on the doping value $x = 0.075$.

A Holstein-Primakoff transformation maps the magnetic Hamiltonian onto a lattice boson Hamiltonian⁵

$$\begin{aligned} \mathcal{H} = & - \sum_{\langle ij \rangle} J_{ij} \left[\sqrt{1 - \frac{n_i}{2}} b_i b_j^\dagger \sqrt{1 - \frac{n_j}{2}} + \text{h.c.} \right] \\ & + \sum_{\langle ij \rangle} J_{ij} (n_i - 1)(n_j - 1) + \sum_i D_i (n_i - 1)^2 \\ & - g\mu_B H \sum_i n_i + \text{const.} \end{aligned} \quad (4)$$

where b_i, b_i^\dagger are bosonic operators with maximum occupation $n_i = 2$; here $J_{ij} = J_{c, \langle ij \rangle}$, J_{ab} depending on the orientation of the bond. The single-ion anisotropy plays the role of an on-site repulsion term for the bosons (which penalizes doubly occupied as well as empty sites, due to the spin-inversion symmetry of the Hamiltonian); the antiferromagnetic couplings play the role of a hopping term as well as of nearest-neighbor repulsion; and the role of the chemical potential is taken by the applied magnetic field. In particular the pure system in zero field is in a Mott-insulating phase with $n = 1$ particle per site (corresponding to zero magnetization on each site), and it exhibits a Mott-insulator/superfluid QPT at a critical field $h_{c1} = g\mu_B H / J_c \approx 1.65$; a second transition from superfluid to $n = 2$ Mott insulator is reached at the upper critical field $h_{c2} = 8.69$. In the presence of Br doping h_{c1} shifts to a lower value $h_{c1} = 0.828(3)$ and the QPT connects a Bose-glass to a superfluid state⁵; h_{c2} is instead weakly affected by Br doping, but the corresponding transition also changes to a Bose-glass-to-superfluid one.

To probe the universal character of some of our findings, we consider as well the case of site dilution of the magnetic lattice of DTN, leading to the following model Hamiltonian

$$\begin{aligned} \mathcal{H}_{\text{sd-DTN}} = & J_c \sum_{\langle ij \rangle_c} \epsilon_i \epsilon_j \mathbf{S}_i \cdot \mathbf{S}_j + J_{ab} \sum_{\langle lm \rangle_{ab}} \epsilon_i \epsilon_j \mathbf{S}_l \cdot \mathbf{S}_m \\ & + D \sum_i \epsilon_i (S_i^z)^2 - g\mu_B H \sum_i \epsilon_i S_i^z. \end{aligned} \quad (5)$$

The Hamiltonian parameters are now set to be homogeneous and equal to those of pure DTN, but the random variables ϵ_i have been introduced, taking the value 0 with probability x and 1 with probability $1 - x$. Here x is the lattice dilution. The phase diagram of the model Eq. 5 has been extensively studied in Ref. 35 for a dilution $x = 0.15$, and it exhibits two superfluid/Bose-glass transitions at fields $h_{c1} \approx 1.94(1)$ and $h_{c2} \approx 8.52(2)$. Site dilution of the lattice of magnetic Ni ions in DTN can be achieved by Cd doping³⁶. Similarly to the case of Br-DTN, a spin-boson transformation maps the spin Hamiltonian Eq. (5) to that of a lattice gas of strongly interacting bosons hopping on a spatially anisotropic cubic lattice with site dilution.

In the following we will mainly focus on the vicinity of the critical points h_{c1} and h_{c2} . As sketched in Fig. 1), for $d = 3$ the $T = 0$ QCPs are the origin of a line of critical temperatures $T_c(g)$ ($g = |h - h_{c1(2)}|$) for the transition to a

superfluid condensed phase. The critical temperature is follow the power-law dependence $T_c(g) \sim g^\phi$. In the pure system, $\phi = 2/3$, stemming from the theory of the diluted Bose gas¹²; this result has also been established experimentally with high accuracy for DTN³⁴. In the disordered case, both experiment and theory find $\phi = 1.1(1)$ for Br-DTN; this result is also confirmed theoretically in site-diluted DTN.³⁵ It is remarkable to observe that other recent experiments on different compounds, expected to exhibit a field-induced Bose-glass/superfluid transition, also report values of ϕ which are compatible with what found in DTN. In particular a $\phi \approx 1$ is compatible with the results on K-doped TiCuCl_3 ,⁴, as commented in Ref. 31 (although Ref. 4 claims that an exponent $\phi \sim 2$ can be extracted from a fit to the experimental data, see also Ref. 32). Values of ϕ compatible with those of doped DTN are also found in a recent experiment on piperazinium- $\text{Cu}_2(\text{Cl}_{1-x}\text{Br}_x)_6$.⁶

This mounting theoretical and experimental evidence in favor of $\phi \approx 1$ for the T_c line stemming from the dirty-boson QCP clashes with the only prediction existing in the literature, namely that of Ref. 8, giving $\phi = \nu z \geq 2$ if $z = d$. In the following section we will shortly review the scaling Ansatz on the free energy of dirty bosons from which the above prediction stems, as well as its further implications for measurable properties.

IV. ONE-ARGUMENT CROSSOVER SCALING ANSATZ

The onset of a finite-temperature transition at $T_c(h)$ starting from the QCPs at h_{c1} , h_{c2} is a complex problem in the theory of critical phenomena, because the thermal transition and the quantum transition are completely different in nature. A comprehensive treatment of the two can be attempted via the crossover scaling theory of phase transitions³⁷, which can account for the crossover between the quantum critical behavior at low and zero temperature and in the vicinity of the QCP, and the classical critical behavior close to the line of critical temperatures $T_c(h)$ (see Fig. 1 for a sketch). For a system of bosons in a disordered environment Ref. 8 propose the simplest possible (*one-argument*) crossover scaling Ansatz for the singular part of the free-energy density, namely

$$f_s(T, g) \sim |g|^{2-\alpha} F\left(\frac{T}{|g|^{\nu z}}\right) = T^{\frac{2-\alpha}{\nu z}} G\left(\frac{T}{|g|^{\nu z}}\right) \quad (6)$$

where $g = h - h_{c1(2)}$ and ν , z and α are the critical exponent of the QCP. Here T is in units of J_c/k_B . Such a scaling Ansatz can be obtained via a phenomenological assumption for the behavior of the free energy under renormalization group (RG)³⁷. Such a behavior is valid when the QCP is a fixed point under RG which only admits the temperature T and the control parameter g as directions of instability. All other directions in parameter space (the strength of disorder, the strength of interactions, etc.) are supposed to be stable directions, and the associated parameters can be eliminated from the scaling Ansatz.

In order for the system to exhibit a finite-temperature transition at T_c , the function $F(y)$ must exhibit a singularity at a

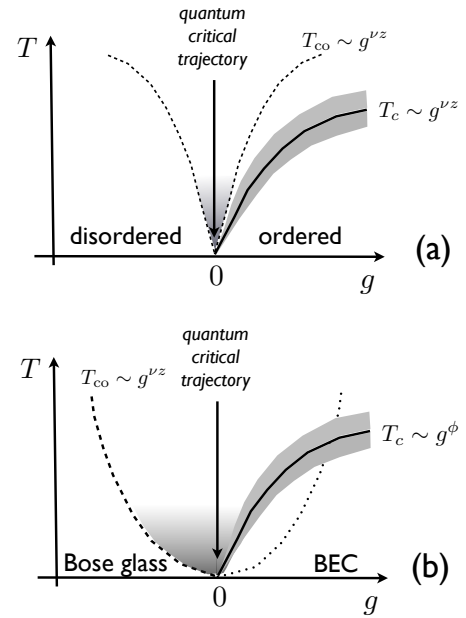


FIG. 1: (a) At a QPT, the quantum critical behavior at finite temperature manifests itself within a "fan" loosely bounded from below by crossover lines $T_{co} \sim g^{\nu z}$. The line of thermal transitions $T_c \sim g^\phi$, and the surrounding Ginzburg region (gray-shaded area) of classical critical behavior, can be well decoupled from the quantum critical fan if $\phi = \nu z$. (b) *Conjectured* picture for the dirty-boson QPT: for dirty bosons $\phi < \nu z$, so that the hierarchy between $T_c(g)$ line and the putative crossover temperature T_{co} to quantum-critical behavior is actually inverted. This would imply that the Ginzburg region and the quantum critical region touch each other.

given value y_c of its argument, so that one expects the critical temperature to follow the scaling law $T_c = y_c |g|^\phi$ with scaling exponent $\phi = \nu z$. This means that, according to the scaling Ansatz Eq. (6), the onset of the critical temperature is completely governed by the critical exponents ν and z of the QPT. Assuming that $z = d$ for the dirty-boson QCP,⁸ and given that $\nu \geq 2/d$ according to the Harris criterion³⁸, one obtains a scaling exponent $\phi = \nu z \geq 2$, as already mentioned previously.

Further consequences of the scaling Ansatz Eq. 6 involve the thermodynamic behavior of the system along the quantum critical trajectory, $T \rightarrow 0$ for $g = 0$. In fact one has that the specific heat C scales as

$$C \sim T \frac{\partial^2 f_s}{\partial T^2} \Big|_{g=0} \sim T^{x_C} \quad (7)$$

with

$$x_C = \frac{2-\alpha}{\nu z} - 1 \quad (8)$$

while the uniform (field-induced) magnetization scales as

$$m(T) - m(0) \sim \frac{\partial f_s}{\partial g} \Big|_{g=0} \sim T^{x_m} \quad (9)$$

with

$$x_m = \frac{1 - \alpha}{\nu z}. \quad (10)$$

The scaling Ansatz Eq. (6) is completely consistent with the validity of conventional scaling at the QCP, and in particular of hyperscaling, $\nu(d+z) = 2 - \alpha$, so that one further obtains $x_C = (d+z)/z - 1 = 1$ and $x_m = 2 - 1/(\nu z) \geq 3/2$.

The prediction $\phi \geq 2$ is based on the assumption that $z = d$, which, as discussed in Sec. II, is still a matter of debate. Hence one could argue that the prediction of Ref. 8 can be reconciled with the observations that $\phi \approx 1$ in disordered magnets by assuming that $z = d$ is indeed violated. In the next section we will provide an accurate study of the quantum critical scaling at the $T = 0$ QCP for both Br-doped DTN and site-diluted DTN, testing the validity of the $z = d$ prediction.

V. FINITE-SIZE SCALING FOR THE BR-DTN HAMILTONIAN

In this section we provide a finite-size scaling analysis of quantum Monte Carlo results for the dirty-boson QCP exhibited by the models for doped DTN (Br-doped or site-diluted). Our quantum Monte Carlo results have been obtained making use of the Stochastic Series Expansion (SSE) approach³⁹ on L^3 lattices with $L = 12, 14, 16$ and 18 . All results are averaged over ~ 300 disorder realizations. The quantities of interest here are: 1) the correlation length along the c axis and in ab plane, obtained via the second-moment estimator

$$\xi_p = \frac{L}{2\pi} \sqrt{\frac{S^\perp(\mathbf{Q})}{S^\perp(\mathbf{Q} + \mathbf{q})} - 1}; \quad (11)$$

where

$$S^\perp(\mathbf{k}) = L^{-3} \sum_{ij} e^{i\mathbf{k} \cdot (\mathbf{r}_i - \mathbf{r}_j)} \langle S_i^x S_j^x + S_i^y S_j^y \rangle \quad (12)$$

is the structure factor for the spin components transverse to the applied field, $\langle \dots \rangle$ denotes the thermal and disorder average, $\mathbf{Q} = (\pi, \pi, \pi)$ is the ordering vector, and $\mathbf{q} = (2\pi/L)\hat{c}$ for $p = c$ and $\mathbf{q} = (2\pi/L)\hat{a}$ (or $(2\pi/L)\hat{b}$) for $p = ab$; 2) the spin stiffness

$$\rho_s = \frac{k_B T}{4J_c L} \langle |\mathbf{W}|^2 \rangle \quad (13)$$

where $\mathbf{W} = (W_a, W_b, W_c)$ is the winding number of bosonic worldlines along the three spatial directions⁴⁰; 3) the squared order parameter, defined as $m_s^2 = S^\perp(\mathbf{Q})/L^3$.

We have applied a β -doubling procedure⁴¹, particularly fit for SSE, which consists in decreasing exponentially the temperature until convergence of the above quantities is reached towards their $T = 0$ value. Fig. 2 shows that, for the system sizes under investigation, this approach leads successfully to the physical $T = 0$ value of the quantities of interest for temperatures $T \approx 2 * 10^{-3} J_c$. In particular Fig. 2 shows that convergence is achieved even in the most delicate case $h = 0.83$

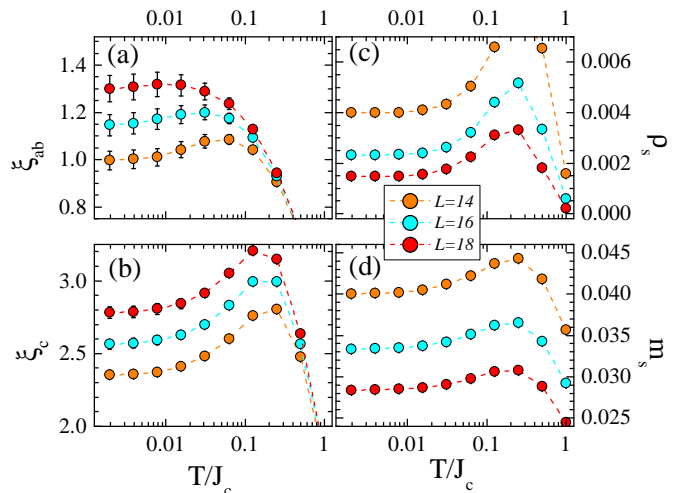


FIG. 2: β -doubling plots for the correlation length, spin stiffness and order parameter of the Br-DTN Hamiltonian, $h = 0.83$.

for Br-doped DTN, corresponding to a field very close to the QCP.

If conventional scaling applies to the system - namely, if $3d$ dirty bosons are below their upper critical dimension - then one expects the following finite-size scaling behavior for the above quantities:

$$\xi_p(g, L) = L F_{\xi_p}(|g|L^{1/\nu}) \quad (14)$$

$$\rho_s(g, L) = L^{d+z-2} F_{\rho_s}(|g|L^{1/\nu}) \quad (15)$$

$$m_s^2(g, L) = L^{2\beta/\nu} F_{m_s}(|g|L^{1/\nu}) \quad (16)$$

For finite-temperature data, one should also include the temperature dependence of the scaling functions as $F_O(|g|L^{1/\nu}, \beta L^{-z})$ for the observable O , and hence one would need a prior knowledge of the z exponent to be able to obtain the universal functions from collapse of the universal data. On the other hand we can omit the temperature argument of the scaling functions, having systematically eliminated thermal effects from our data; this will allow us to give an unbiased estimate of the critical exponents.

A. Br-doped DTN

We can make use of Eq. (14) to locate the critical field via the intersection of the ξ_p/L curves plotted as a function of h . This is shown in Fig. 3. The crossing point for the ξ_{ab}/L curves is located at $h_{c1} = 0.830(15)$, with a fairly large error bar due to the shallow form of the curves around the critical field. In particular this value is in very good agreement with the value $h_{c1} = 0.828(3)$ obtained by extrapolation of the $T_c(h)$ curve to zero temperature⁵. On the other hand, we observe that the crossing point for the ξ_c/L curves is at a slightly larger value, $h_{c1} = 0.850(5)$. We attribute

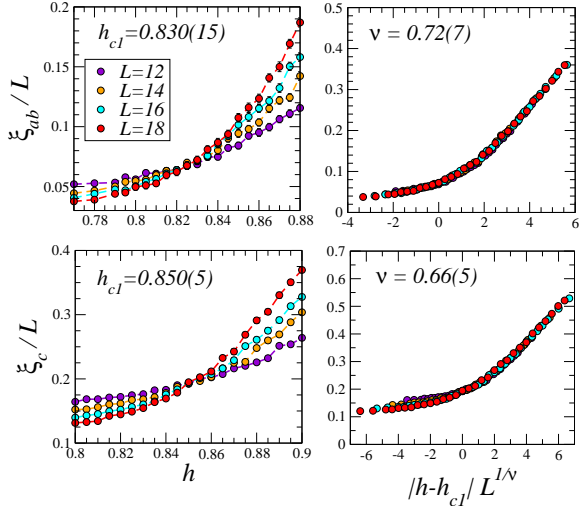


FIG. 3: Scaling plots of the QMC data for the correlation length of the Br-DTN model.

this discrepancy to the spatial anisotropy present in the Br-DTN model in terms of disorder effects, given that bond randomness only affects the J_c couplings and not the J_{ab} ones. This asymmetry might hinder the development of correlations along the c axis, and hence alter the finite-size estimates of the critical field. Nonetheless a very good collapse is obtained in a scaling plot as a function of $gL^{1/\nu}$ with $\nu = 0.72(7)$ for the ξ_{ab} curves and $\nu = 0.66(5)$ for the ξ_c curves (only for positive g for the latter, again showing an asymmetry between the two spatial directions).

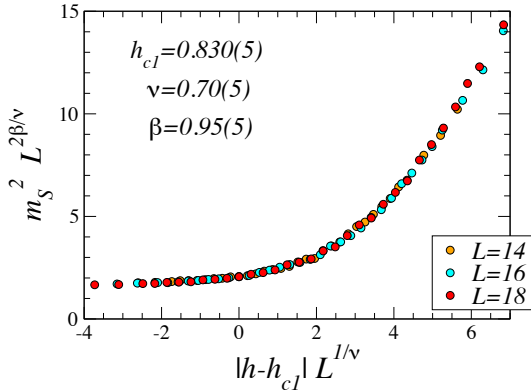


FIG. 4: Scaling plots of the QMC data for the squared order parameter of the Br-DTN model.

To better refine our estimate of h_{c1} we consider the scaling of the order parameter, depicted in Fig. 4. We observe an excellent collapse for $h_{c1} = 0.830(5)$, $\nu = 0.70(5)$ and $\beta = 0.95(5)$. On the other hand, we cannot obtain such a good collapse both for negative and positive g values by using the larger h_{c1} estimate given by the scaling of ξ_c . Hence in the following we will make use of the $h_{c1} \approx 0.83$ esti-

mate. We conclude this analysis by examining the behavior

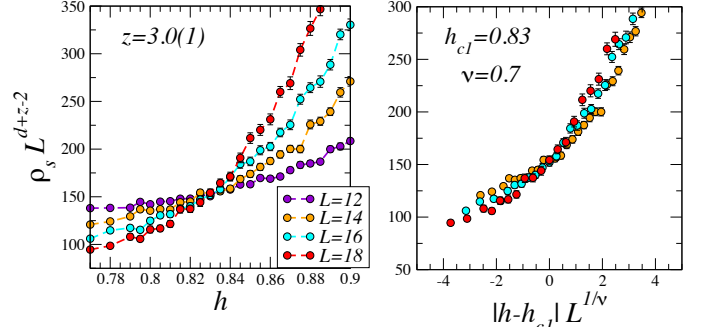


FIG. 5: Scaling plots of the QMC data for the spin stiffness of the Br-DTN model.

of ρ_s . Imposing that the $\rho_s L^{d+z-2}$ curves cross at the estimated h_{c1} , we obtain that $z = 3.0(1)$, fully consistent with $z = d$ (see Fig. 5). A full scaling plot of ρ_s with $\nu \approx 0.7$ does not give a very satisfactory collapse far from the critical point. We attribute this lack of scaling to the asymmetry between the ab plane and the c axis: indeed ρ_s contains the winding number fluctuations along all spatial directions, whose scaling properties for the sizes we have examined might be different. We postpone to future work a detailed analysis of the winding number fluctuations along specific spatial directions. Another possibility is that corrections to scaling must be taken into account in the behavior of ρ_s for the system sizes considered here (although they did not seem necessary to account for the scaling of the other observables).

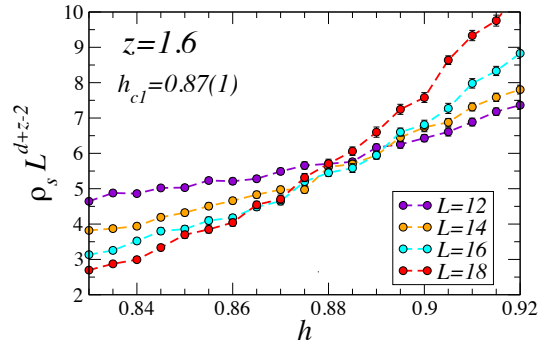


FIG. 6: Scaling plot of the QMC data for the spin stiffness of the Br-DTN model using $z = 1.6$. The scaled curves do not appear to cross at the same field.

Relying on the conclusions of Sec. IV, one would argue that $\nu z = \phi$ would rather imply that $z = \phi/\nu \approx 1.6$ (using $\phi = 1.1$ and $\nu = 0.7$). On the other hand, when using this value for z we obtain that the $\rho_s(L)L^{d+z-2}$ curves do not cross at one and the same critical field – see Fig. 6. Willing to identify an estimate of the critical field from the crossing of the two largest system sizes ($L = 16$ and 18) we obtain

$h_{c1} = 0.87(1)$, clearly inconsistent with the previous estimates. Hence the equality $\phi = \nu z$ is definitely incompatible with our results.

B. Site-diluted DTN

We can repeat a similar analysis to that of Br-doped DTN for QMC results on site-diluted DTN with $x = 0.15$ dilution. All results are summarized in the scaling plots of Fig. 7, referring to the case of both h_{c1} and h_{c2} . The central result is that all critical exponents appear to be consistent between the two transitions. In the case of site dilution, the asymmetry between the ab plane and c axis in terms of the disorder distribution is absent, and indeed we do not observe a significant discrepancy in the critical fields estimated via ξ_{ab} and ξ_c ; moreover we obtain a good collapse of the ρ_s data, unlike what observed in Br-DTN.

Even more importantly, the critical exponents estimated for site-diluted DTN are fully consistent with the estimates obtained above for Br-doped DTN, as well as with the estimates of Ref. 23 for the Bose-Hubbard model with a random chemical potential. The latter reference gives $\nu = 0.70(12)$, $z = 3$, and $\eta \approx -1$, from which we can extract $\beta = \nu(d + z - 2 + \eta)/2 \approx 1.05$. Hence we can conclude that none of the results obtained so far are specific of the kind of disorder we have considered, and that they rather reflect the universal behavior of interacting bosons in $d = 3$ in the presence of short-range correlated disorder.

VI. THERMODYNAMICS ALONG THE QUANTUM CRITICAL TRAJECTORY OF BR-DTN: NUMERICS AND EXPERIMENT

A further test of the crossover scaling Ansatz comes from the direct determination of the exponents x_C and x_m from numerical simulations and experiments. In the following we describe the extraction of these exponents from our quantum Monte Carlo simulations close to the h_{c1} critical field for the Br-DTN Hamiltonian, as well as from specific heat experiments on Br-DTN.

A. Quantum Monte Carlo

In Fig. 8 we analyze the scaling of the energy per spin, $E(T)$, as obtained from our QMC simulations. The thermal energy is expected to scale as a power law close to the QCP, $E(T) = E(0) + A_E T^{x_E}$ where $x_E = x_C + 1$. We fit our QMC data for two field values close to the estimated $h_{c1} = 0.828(3)$ T value, $h_{c1} - 0.04$ T and $h_{c1} + 0.007$ T, and for two system sizes, $L = 14$ and $L = 18$. We make use a windowing technique, extracting the fitting parameters over a decreasing temperature window $[0, T]$ in order to obtain the asymptotic quantum critical behavior for $T \rightarrow 0$. The results of this fitting procedure are shown in Fig. 8. For both system sizes and field values we obtain that the x_E estimate

converges to a value $x_E = 2.8(2)$ as the temperature window for the fit is progressively reduced, whence we extract the estimate $x_C = 1.8(2)$.

A similar procedure is used to analyze the magnetization $m(T)$, which is fitted to the form $m(T) = m(0) + A_m T^{x_m}$ where A_m is a constant. The result of the windowing analysis is shown in Fig. 9, yielding an exponent $x_m = 1.8(1)$.

B. Specific heat measurements

We can perform a similar analysis to the experimental specific heat data of Br-doped DTN close to the experimental H_{c1} value, $H_{c1} = 1.07(1)$, namely for $H = 1, 1.1$ and 1.2 T. The specific heat has been measured in a dilution refrigerator using the quasi-adiabatic heat pulse method. The analysis of the low- T experimental data for the specific heat is complicated by the appearance of a nuclear Schottky anomaly, which introduces a term that scales roughly as H^2/T^2 in the specific heat - at least at sufficiently small fields - as already observed in pure DTN.^{42,43} The Schottky anomaly contribution to the specific heat at H_{c2} swamps the low- T electronic contribution, and thus we focus on data near H_{c1} .

We fit the specific heat data to the form

$$C(T) = \left(\frac{a_n H}{T}\right)^2 [1 - \tanh^2(b_n H/T)] + a_e T^{x_C} \quad (17)$$

where the first term mimics the temperature behavior of the specific heat of paramagnetic nuclear spins, and the second term is the electron-spin contribution. In particular, we fit the specific heat data at $H = 1.1$ T over a variable temperature range $[0, T]$ using the same windowing technique as for the theoretical data (see Fig. 10(b)). This gives us stable fit parameters as T is lowered, and for $T = 0.6$ K we obtain a very good fit with $a_n = 0.0155(2)$ [JK/(T²mol)]^{1/2}, $b_n = 0.034(2)$ K/T, $a_e = 1.004(7)$ J/(K^{1+x_C} mol) and $x_C = 2.00(1)$ (see Fig. 10(a)).

The other data sets are instead fit differently: we use as fitting parameters a_e and x_C only, while a_n and b_n are kept fixed - as the nuclear contribution depends explicitly on the field. For $H = 1.0$ T we obtain $a_e = 1.03(1)$ J/(K^{1+x_C} mol) and $x_C = 2.15(1)$, while for $H = 1.2$ T we find $a_e = 1.004(1)$ J/(K^{1+x_C} mol) and $x_C = 1.89(1)$ - see Fig. 10(c-d). For both fields the nuclear part is quantitatively reproduced by using the explicit field dependence of Eq. (17). In particular for $H = 1.2$ T the experimental data deviate significantly from the fitting form for $T \approx 0.2$ K, due to the apparition of an anomaly associated with the onset of long-range order in the electronic spins (the value of $T_c \approx 0.2$ K at $H = 1.2$ T is in good agreement with the $T_c(H)$ curve reported in Ref. 5). Nonetheless above T_c the specific heat appears to follow a power-law scaling characteristic of the quantum-critical behavior.

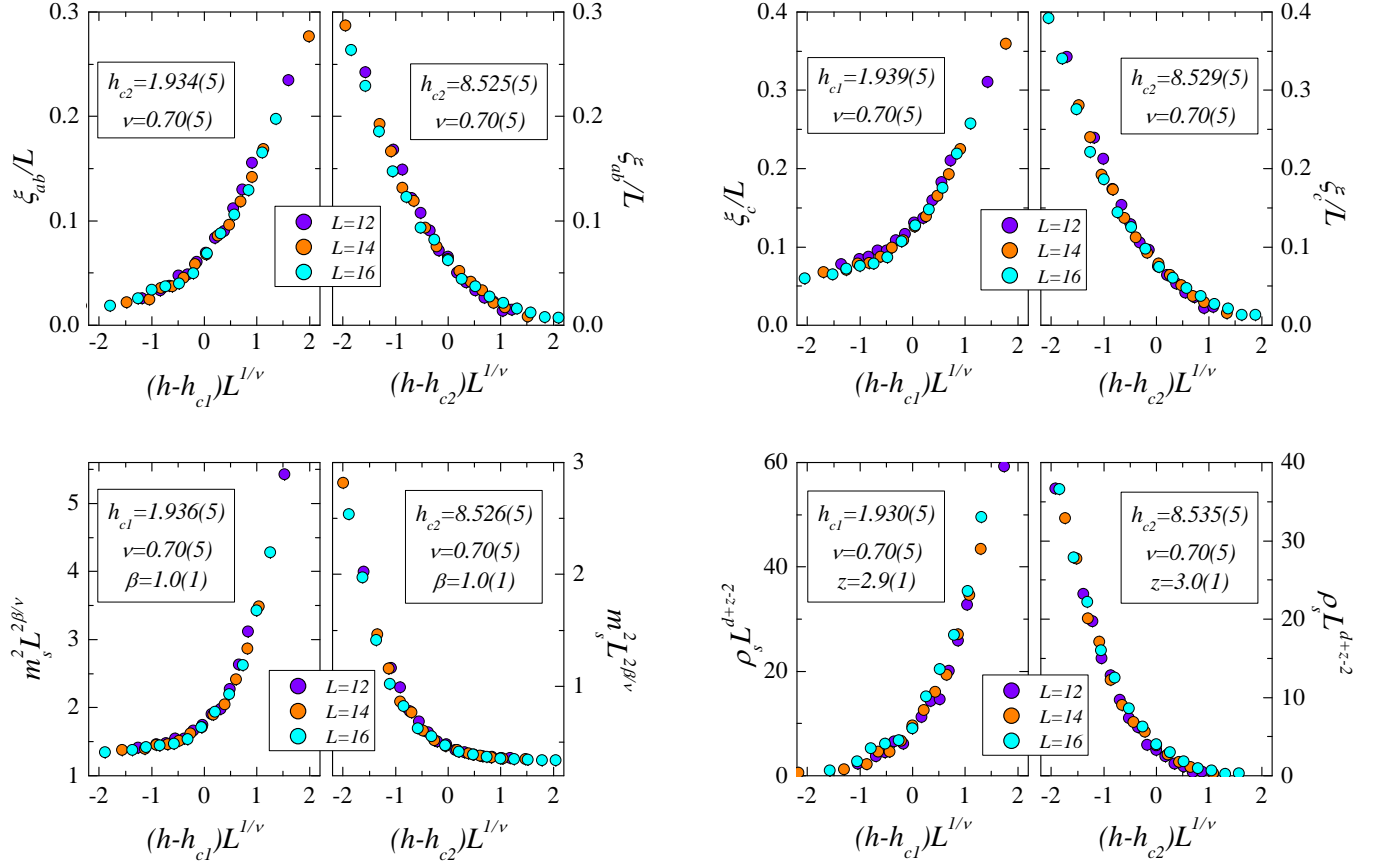


FIG. 7: Scaling plots for the site-diluted DTN Hamiltonian with dilution $x = 0.15$.

C. Discussion

The specific heat exhibits a power-law behavior along the quantum critical trajectory with an exponent $x_C = 1.8 - 2$ determined both by numerical simulations and by experiments on Br-DTN. Such an exponent is a clear signature of the quantum critical behavior, as it clearly differs from the power-law behavior with $x_C = 3$ appearing in the BEC phase⁵. Moreover, this result is inconsistent with the prediction $x_C = 1$ coming from the scaling Ansatz Eqs. (6) and Eq. (8) with $z = d$. The magnetization also exhibits a distinct quantum critical behavior with exponent $x_m \approx 1.8$. Such a behavior is markedly different from that exhibited in the BEC regime, in which the thermal magnetization initially decreases as $-T^{3/2}$ when T grows above zero¹². In turn the quantum critical exponent x_m found with QMC is not consistent with the prediction $x_m \approx 1.5$ from Eqs. (6) and Eq. (10) with $z = d$ and $\nu \approx 0.7$. These results, together with the value $\phi = 1.1(1)$, call for a revision of the scaling behavior of the free energy governing the region around the QCP.

VII. GENERALIZED SCALING ANSATZES

As already mentioned in Sec. II, the long-wavelength effective action describing the physics of dirty bosons around the QCP does not lend itself to a well controlled RG analysis, due to the non-perturbative role of disorder, and to the fact that the upper critical dimension appears to be $d_c = \infty$.^{7,8} Therefore an educated guess of the scaling Ansatz for the free energy is not straightforward. In the following we discuss two attempts at a generalization of the scaling Ansatz, Eq. (6), based on the possible presence of a dangerously irrelevant term in the effective action, namely a direction in parameter space which cannot be simply eliminated in the RG flow. We cannot say a priori whether the term in question is represented by the interaction or by the disorder, or by a combination of the two. The generalization of the scaling Ansatz, although introduced in a heuristic way, can lead to relationships between the critical exponents which are compatible with the numerical and experimental values cited above for Br-DTN. A fully consistent picture with our results can only be obtained if a dangerously irrelevant operator enters in a *weak* way in the scaling, only affecting the finite-temperature behavior.

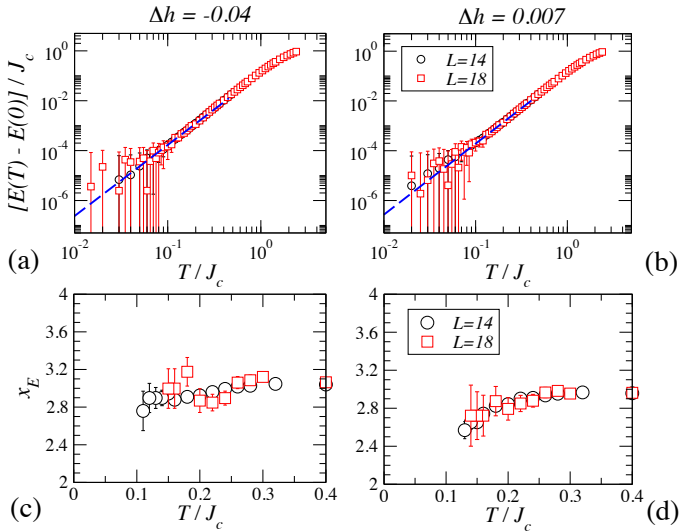


FIG. 8: (a)-(b) Thermal energy $E(T) - E(0)$ of the Br-DTN Hamiltonian close to the lower critical field h_{c1} . The dashed lines correspond to a fit with $x_E = 2.85$; (c)-(d) x_E exponent obtained by fitting the data in (a)-(b) over a temperature window $[0, T]$.

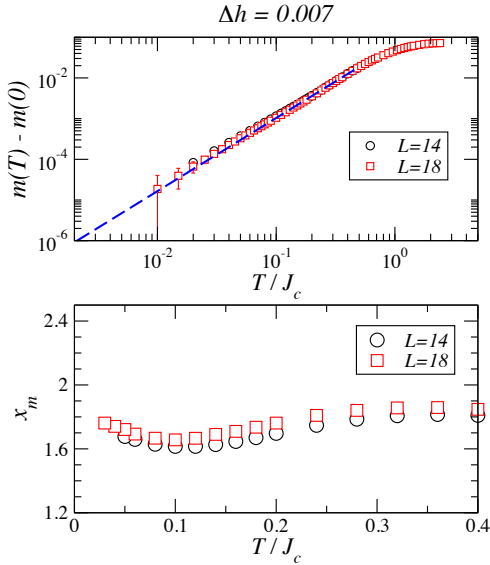


FIG. 9: Upper panel: thermal magnetization of the Br-DTN Hamiltonian close to the lower critical field h_{c1} ; the dashed line corresponds to a fit with $x_m = 1.8$. Lower panel: x_m exponent obtained by fitting the $m(T)$ data over a temperature window $[0, T]$.

A. Scaling Ansatz in presence of a dangerously irrelevant term

We consider the free energy density $f_s(g, T, u)$, depending on the distance g to the critical point, the temperature T and the coefficient of a dangerously irrelevant term u . Close to the QCP, f_s is assumed to scale under m cycles of an RG transformation – scaling the spatial dimensions by a factor b

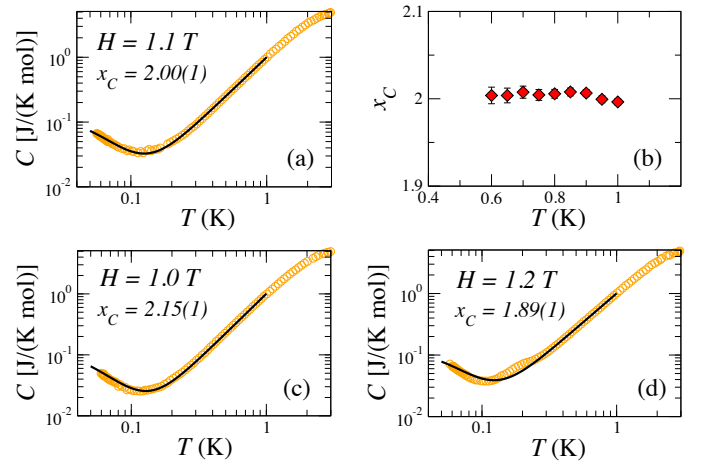


FIG. 10: Specific heat of Br-DTN close to the lower critical field H_{c1} . The solid lines are fits as described in the text.

and the imaginary-time dimension by a factor $b^z - \text{as}$

$$f_s(g, T, u) \approx b^{-m(d+z)} f_s(g b^{m y_g}, T b^{m y_T}, u b^{-m y_u}) . \quad (18)$$

where y_g , y_T and $y_u > 0$. Stopping the RG flow when $g b^{m y_g} \approx 1$, namely when the correlation length is renormalized to order 1, $\xi/b^m \sim 1$ with $y_g = 1/\nu$, and identifying $y_T = z$, one obtains the standard scaling Ansatz

$$f_s(g, T, u) \approx g^{\nu(d+z)} \Phi\left(\frac{T}{g^{\nu z}}, u g^{\nu y_u}\right) . \quad (19)$$

Letting $u \rightarrow 0$ leads to singularities in f_s or in its derivatives. Following Ref. 44 one can assume that $\Phi(y_1, y_2)$ has a singularity when $y_2 \rightarrow 0$, in the form

$$\Phi(y_1, y_2) \approx A(y_1 y_2^\rho) y_2^{-\mu} \quad (20)$$

where ρ and μ are unknown exponents, except for the fact that $\mu > 0$. This assumption immediately leads to the scaling Ansatz

$$f_s(g, T, u) \approx g^{2-\alpha} A\left(\frac{T}{g^\phi} u^\rho\right) \quad (21)$$

where $2 - \alpha = \nu(d+z) - \nu y_u \mu \leq \nu(d+z)$ (in possible violation of hyperscaling) and $\phi = \nu z - \rho y_u \nu \leq \nu z$ (if $\rho > 0$). Analogously to what discussed in Sec. IV, the thermal critical line must correspond to a singularity in $A(y)$ at y_c , so that $T_c \sim g^\phi$. The inequality $\phi \leq \nu z$ is clearly verified by our numerical and experimental values for the ϕ , ν and z exponents of Br-DTN.

Rewriting Eq. (21) as

$$f_s(g, T, u) \approx T^{\frac{2-\alpha}{\phi}} u^{\frac{\rho(2-\alpha)}{\phi}} B\left(\frac{g}{T^{1/\phi} u^{\rho/\phi}}\right) \quad (22)$$

and applying Eqs. (7) and (9), one obtains the following exponents for the along the quantum critical trajectory

$$x_m = \frac{1-\alpha}{\phi} \quad x_C = x_m + \frac{1}{\phi} - 1 \quad (23)$$

Due to the violation of hyperscaling, α is a priori unknown. One can determine α by imposing that $x_m = 1.8(1)$, obtaining $\alpha = -0.98(1)$, and hence $x_C = 1.7(3)$, in good agreement with the value obtained numerically and experimentally for Br-DTN.

Yet the above result has the major drawback of requiring a strong violation of hyperscaling at the QPT, $2 - \alpha \leq \nu(z+d)$. Violation of hyperscaling is in open contradiction with the analysis of Sec. V, which is successfully based on conventional scaling forms for a QPT below the upper critical dimension. This suggests that a possible dangerously irrelevant operator enters in a more subtle way, leaving the quantum critical behavior unaffected and only manifesting itself in the finite-temperature singularity of the free energy.

B. Continentino's scaling

The previous scaling Ansatz, albeit giving the prediction Eq. (23) which is fully compatible the exponents for Br-DTN, is not the most general Ansatz in presence of a dangerously irrelevant term (as also pointed out in Ref. 44). In the absence of disorder, the boson-boson interaction is known rigorously to play the role of a dangerously irrelevant term⁸, and yet Eq. (23) is not satisfied: indeed one has that $\phi = 2/3$ (see Ref. 12) and $\alpha = 0$ (Gaussian fixed point), leading to $x_C = 2$, while the exact result is $x_C = 3/2$, as also measured experimentally in undoped DTN.⁴²

Continentino⁴⁵ has proposed an alternative scaling Ansatz to describe the singular part of the free energy close to the classical critical line (namely in the so-called Ginzburg region, see Fig. 1) in the presence of a dangerously irrelevant term:

$$f_s(g, T, u) \approx \tilde{g}(T)^{2-\alpha} \Psi \left(\frac{T}{\tilde{g}(T)^{\nu z}} \right) \quad (24)$$

where $\tilde{g}(T) = g - uT^{1/\phi}$ is the distance to the thermal critical value of the control parameter, shifted with respect to its $T = 0$ value g . The function $\Psi(t)$ is supposed to have the following properties: 1) $\Psi(t \rightarrow 0) = \text{const.}$, so that the Ansatz reproduces the conventional quantum critical behavior $f_s \sim g^{2-\alpha}$ at $T = 0$; 2) $\Psi(t \rightarrow \infty) \sim t^x$, where $x = (\alpha_T - \alpha)/(\nu z)$, and α_T is the critical exponent of the thermal transition, so that $f_s \sim |\tilde{g}(T)|^{2-\alpha_T}$ when approaching the thermal critical line. In particular in the above Ansatz the operator u disappears from the scaling when $T \rightarrow 0$, leaving the QPT unaffected. Hence hyperscaling can be safely assumed at $T = 0$.

In general Eq. (24) is only guaranteed to work in the Ginzburg region⁴⁶, but one can test the consequences of its extension to a broader range of validity, including the quantum critical trajectory, as done in Ref. 45. Using hyperscaling at both the classical and quantum phase transition, this leads to the predictions

$$x_C = \nu_T d \left(\frac{1}{\phi} - \frac{1}{\nu z} \right) + \frac{d}{z} \quad (25)$$

and

$$x_m = x_C + 1 - \frac{1}{\phi} \quad (26)$$

where ν_T is the critical exponent at the thermal transition.

Using $\phi = 1.1(1)$, $\nu = 0.70(5)$, $z = d$ and $\nu_T = 0.669(1)$ for the 3DXY universality class⁴⁷, we obtain $x_C = 1.9(2)$ and $x_m = 2.0(2)$, fully compatible with our numerically and experimentally determined values.

A possible argument can be formulated to justify the apparent success of the above Ansatz *a posteriori*. This Ansatz implies the rather unconventional situation, Eq. (25), in which both the quantum and the classical critical exponents enter in the scaling along the quantum critical trajectory⁴⁶. This is not what one would typically expect, given that the classical critical exponents pertain to the Ginzburg region, while the quantum critical exponent pertain to the quantum critical fan above the QCP. The Ginzburg region surrounds the classical critical line $T_c \sim |g|^\phi$, while the quantum critical fan is (loosely) lower bounded by a crossover line $T_{co} \sim g^{\nu z}$ reflecting the typical energy scale of the spectral features which vanish at the QCP. If $\phi = \nu z$, as predicted by conventional scaling, Eq. (6), the two above regions can be well separated (Fig. 1(a)). On the other hand, if $\phi < \nu z$ (as in the dirty-boson case, in which $\nu z \approx 2\phi$) the quantum critical regime is not lower-bounded by T_{co} but rather by T_c , and hence the quantum-critical region and the Ginzburg region are completely contiguous, so that one could imagine that the quantum critical trajectory could be influenced by the classical critical behavior (Fig. 1(b)). This very unconventional scenario is purely speculative at this stage, and it will require more investigations⁴⁸.

C. Alternative scaling

To avoid the shortcomings of Continentino's scaling - namely the extension to the quantum-critical trajectory of a scaling form expected to be valid close to the classical critical line only - we can propose a further scaling Ansatz which generalizes Continentino's one while preserving its virtues. Indeed Eq. 24 is consistent with the more general, *two-argument* scaling Ansatz

$$f_s(T, g, u) \approx g^{\nu(d+z)} \mathcal{G} \left(\frac{g}{T^{1/(\nu z)}}, u T^{\frac{1}{\phi} - \frac{1}{\nu z}} \right). \quad (27)$$

To obtain hyperscaling at $T = 0$, we simply need to assume that $\mathcal{G}(y_1, y_2) \rightarrow \text{const.}$ when $y_1 \rightarrow \infty$ and $y_2 \rightarrow 0$.

We rewrite the above scaling form as

$$f_s(T, g, u) \approx T^{\frac{d+z}{z}} \mathcal{F} \left(\frac{g}{T^{1/(\nu z)}}, u T^{\frac{1}{\phi} - \frac{1}{\nu z}} \right) \quad (28)$$

where $\mathcal{F} \rightarrow (g/T^{1/(\nu z)})^{\nu(d+z)} \mathcal{G}$ when approaching the QCP at very low temperatures, namely $T \rightarrow 0$ and $g \rightarrow 0$ but $g/T^{1/(\nu z)} \rightarrow \infty$ (implying $T \ll T_{co} \sim g^{\nu z}$).

On the other hand, when approaching the quantum-critical trajectory, $T \rightarrow 0$, $g \rightarrow 0$, but $g/T^{1/(\nu z)} \rightarrow 0$ (namely

$T \gg T_{co} \sim g^{\nu z}$), we assume a rather different form for the \mathcal{F} function, namely

$$\mathcal{F}(y_1, y_2) \approx y_2^\theta (f_1 y_1 + f_2 y_2 + \dots) \quad (29)$$

when $y_1, y_2 \rightarrow 0$ (f_1 and f_2 are constants)⁴⁹. Upon this assumption we readily obtain that, along the quantum-critical trajectory $y_1 = 0, y_2 \rightarrow 0$

$$x_C = \frac{d+z}{z} + (\theta+1) \left(\frac{1}{\phi} - \frac{1}{\nu z} \right) - 1 \quad (30)$$

and

$$x_m = x_C - \frac{1}{\phi} + 1. \quad (31)$$

The θ exponent can be determined by Eq. (30), $\theta \approx 0.9$, using the numerical values of all the other exponents. Hence we can obtain a picture which is globally consistent with all of our results.

VIII. CONCLUSIONS

We have investigated, both theoretically and experimentally, the field-induced quantum phase transition in the magnetic Hamiltonian of DTN in the presence of bond/anisotropy disorder or of site dilution. This quantum phase transition represents a well controlled realization of the dirty-boson quantum critical point (QCP) in three dimensions. We have provided compelling evidence that conventional scaling is obeyed at the dirty-boson QCP, but that unconventional scaling (including the possible presence of a dangerously irrelevant operator) is necessary to account for the thermodynamics along

the quantum critical trajectory, as well as for the power-law dependence of the line of critical temperatures on the applied field. Our results are compatible with the prediction $z = d$, but incompatible with the prediction $\phi = \nu z$ for the exponent of the power-law scaling of the critical temperature, as also found in recent experiments^{4-6,31,32}. Within a generalized scaling Ansatz ϕ plays the role of an independent exponent, whose value, combined with that of quantum critical exponents as well as classical critical ones, can be quantitatively related to the exponents governing the power-law scaling of the specific heat and of the magnetization along the quantum critical trajectory. A recent experiment on piperazinium-Cu₂(Cl_{1-x}Br_x)₆ has measured the order-parameter exponent via neutron scattering at low temperature,⁶ giving $\beta \approx 0.5$. Our evidence is that this exponent is not compatible with the dirty-boson universality class in $d = 3$ (see also Ref. 23); more investigations will be necessary in this direction.

While a conclusive picture on the dirty-boson quantum critical point is still far from obvious, our results provide a quantitative scenario which a well-controlled theory of the dirty-boson effective action⁸ should be able to reproduce. More generally, our results further confirm that disordered quantum magnets represent an invaluable tool for the investigation of complex phenomena of interacting bosons, and that they stand among the best candidate systems to unveil the universal features of dirty bosons.

IX. ACKNOWLEDGEMENTS

We thank Qimiao Si for bringing Ref. 46 to our attention. R. Y and T. R. acknowledge support of the DOE (INCITE award).

-
- ¹ P. A. Crowell, F. W. Van Keuls, and J. D. Reppy, Phys. Rev. B **55**, 12620 (1997).
² L. Sanchez-Palencia and M. Lewenstein, Nature Phys. **6**, 87 (2010).
³ T. Hong, A. Zheludev, H. Manaka, and L.-P. Regnault, Phys. Rev. B **81**, 060410(R) (2010).
⁴ F. Yamada, H. Tanaka, T. Ono, and H. Nojiri, Phys. Rev. B **83**, 020409 (2011).
⁵ R. Yu, L. Yin, N. S. Sullivan, J. S. Xia, C. Huan, A. Paduan-Filho, N. F. Oliveira Jr., S. Haas, A. Steppke, C. F. Miclea, F. Weickert, R. Movshovich, E.-D. Mun, B. S. Scott, V. S. Zapf, T. Roscilde, arXiv:1109.4403 (2011).
⁶ D. Hüvonen, S. Zhao, M. Månsson, T. Yankova, E. Ressouche, C. Niedermayer, M. Laver, S. N. Gvasaliya, and A. Zheludev, arXiv:1201.6143 (2012).
⁷ P. B. Weichman, Mod. Phys. Lett. B **22**, 2623 (2008).
⁸ M. P. A. Fisher, P. B. Weichman, G. Grinstein, and D. S. Fisher, Phys. Rev. B **40**, 546 (1989).
⁹ P. B. Weichman and R. Mukhopadhyay, Phys. Rev. Lett. **98**, 245701 (2007).
¹⁰ A. Griffin, T. Nikuni, and E. Zaremba, *Bose-condensed gases at finite temperatures*, Cambridge, 2009.
¹¹ S. Sachdev, *Quantum phase transitions*, Cambridge, 1999.
¹² T. Nikuni, M. Oshikawa, A. Oosawa, and H. Tanaka, Phys. Rev. Lett. **84**, 5868 (2000).
¹³ T. Giamarchi and H. J. Schulz, Phys. Rev. B **37**, 325 (1988).
¹⁴ G. Parisi, arXiv:1201.5813 (2012).
¹⁵ A. Priyadarshie, S. Chandrasekharan, J.-W. Lee, and H. U. Baranger, Phys. Rev. Lett. **97**, 115703 (2006).
¹⁶ H. Meier and M. Wallin, Phys. Rev. Lett. **108**, 055701 (2012).
¹⁷ N. Prokof'ev and B. Svistunov, Phys. Rev. Lett. **92**, 015703 (2004).
¹⁸ S. G. Söyler, M. Kiselev, N. V. Prokof'ev, and B. V. Svistunov, Phys. Rev. Lett. **107**, 185301 (2011).
¹⁹ F. Lin, E. Sørensen, and D. M. Ceperley, Phys. Rev. B **84**, 094507 (2011).
²⁰ T. Roscilde, Phys. Rev. B **74**, 144418 (2006).
²¹ R. Yu, T. Roscilde and S. Haas, New J. Phys. **10** 013034 (2008).
²² R. Yu, O. Nohadani, S. Haas, and T. Roscilde, Phys. Rev. B **82**, 134437 (2010).
²³ P. Hitchcock and E. S. Sørensen, Phys. Rev. B **73**, 174523 (2006).
²⁴ T. Giamarchi, *Quantum physics in one dimension*, Clarendon, Oxford (2004).
²⁵ L. Wang, K. S. D. Beach, and A. W. Sandvik, Phys. Rev. B **73**,

- 014431 (2006).
- ²⁶ O. Nohadani, S. Wessel, and S. Haas, Phys. Rev. B **72**, 024440 (2005).
- ²⁷ F. Alet and E. S. Sørensen, Phys. Rev. B **70**, 024513 (2004).
- ²⁸ T. Giamarchi, C. Rüegg, and O. Tchernyshyov, Nature Phys. **4**, 198 (2008).
- ²⁹ T. Roscilde and S. Haas, Phys. Rev. Lett. **95**, 207206 (2005).
- ³⁰ O. Nohadani, S. Wessel, and S. Haas, Phys. Rev. Lett. **95**, 227201 (2005).
- ³¹ A. Zheludev and D. Hüvonen, Phys. Rev. B **83**, 216401 (2011).
- ³² F. Yamada, H. Tanaka, T. Ono, and H. Nojiri, Phys. Rev. B **83**, 216402 (2011).
- ³³ S. A. Zvyagin, J. Wosnitza, C. D. Batista, M. Tsukamoto, N. Kawashima, J. Krzystek, V. S. Zapf, M. Jaime, N. F. Oliveira, Jr., and A. Paduan-Filho, Phys. Rev. Lett. **98**, 047205 (2007).
- ³⁴ L. Yin, J. S. Xia, V. S. Zapf, N. S. Sullivan, and A. Paduan-Filho Phys. Rev. Lett. **101**, 187205 (2008).
- ³⁵ R. Yu, S. Haas, and T. Roscilde, Europhys. Lett. **89**, 10009 (2010).
- ³⁶ L. Yin, J.S. Xia, N.S. Sullivan, V. S. Zapf, A. Paduan-Filho, R. Yu, and T. Roscilde, Proceedings of the LT26 Conference, to appear on J. Phys: Conf. Ser.
- ³⁷ J. Cardy, *Scaling and Renormalization in Statistical Physics*, Cambridge, 1996, Chap. 4.
- ³⁸ J. T. Chayes, L. Chayes, D. S. Fisher, and T. Spencer, Phys. Rev. Lett. **57**, 2999 (1986).
- ³⁹ O. F. Syljuåsen and A. W. Sandvik, Phys. Rev. E **66**, 046701 (2002).
- ⁴⁰ E. L. Pollock and D. C. Ceperley, Phys. Rev. B **36**, 8343 (1987).
- ⁴¹ A. W. Sandvik, Phys. Rev. B **66**, 024418 (2002).
- ⁴² Y. Kohama, A. V. Sologubenko, N. R. Dilley, V. S. Zapf, M. Jaime, J. A. Mydosh, A. Paduan-Filho, K. A. Al-Hassanieh, P. Sengupta, S. Gangadharaiah, A. L. Chernyshev, and C. D. Batista, Phys. Rev. Lett. **106**, 037203 (2011).
- ⁴³ F. Weickert, R. Kuechler, A. Steppke, L. Pedrero, M. Nicklas, M. Brando, F. Steglich, M. Jaime, V. S. Zapf, A. Paduan-Filho, K. A. Al-Hassanieh, C. D. Batista, and P. Sengupta, arXiv:1204.3064 (2012).
- ⁴⁴ M. E. Fisher in *Critical Phenomena*, Lecture Notes in Physics 186, Springer, Berlin (1983).
- ⁴⁵ M. A. Continentino, *Quantum Scaling in Many-Body Systems*, World Scientific, Singapore, 2001.
- ⁴⁶ L. Zhu, M. Garst, A. Rosch, and Q. Si, arXiv:cond-mat/0408230.
- ⁴⁷ A. Pelissetto and E. Vicari, Phys. Rep. **368**, 549 (2002).
- ⁴⁸ Indeed a similar picture is *a priori* obtained in the pure system, in which $\nu z = 1 > \phi = 2/3$. Nonetheless Continentino's scaling does not apply to the Gaussian quantum critical point of the pure system, as it predicts *e.g.* the wrong x_C exponent.
- ⁴⁹ One can reconcile the two limiting cases of Eq. (27) and Eq. (29) by assuming that \mathcal{F} is a linear combination of the two expressions, given that the first will dominate over the second when approaching the QCP from low temperatures, while the second one will dominate close to the quantum-critical trajectory. On the other hand, the behavior in the Ginzburg region *à la* Continentino can be reproduced by the \mathcal{G} function term, while the contribution of Eq. (29) in that region would be marginal.